Energy & Environmental Science

Accepted Manuscript

ROYAL SOCIETY OF CHEMISTRY

www.rsc.org/ees

Dye-sensitized solar cells with inkjet-printed dyes

Syed Ghufran Hashmi [a], *Merve Özkan* [b], *Janne Halme** [a], *Shaik Mohammed Zakeeruddin* [c], *Jouni Paltakari* [b], *Michael Grätzel* [c], *Peter. D. Lund* [a]

[a] Department of Applied Physics, Aalto University School of Science, P.O. BOX 15100, FI-00076 Aalto (Espoo), Finland

[b] Department of Forest Products Technology, Aalto University School of Chemical Technology, P.O. BOX 15100, FI-00076 Aalto (Espoo), Finland

[c] Laboratory of Photonics and Interfaces, Ecole Polytechnique Federale de Lausanne (EPFL), CH G1 551, Station 6, CH-1015 Lausanne – Switzerland.

Corresponding author's email address:

janne.halme@aalto.fi

Keywords: Dye-sensitized solar cells, inkjet printing, dye sensitization, dye adsorption, dye loading, stability, aging.

Abstract

The slow process in which the light absorbing dye molecules are adsorbed from solution on the nanocrystalline TiO_2 photoelectrode film has been a handicap to fast and cost-effective fabrication of dye-sensitized solar cells (DSSC) with printing techniques. Here, we report a versatile dye sensitization process, achieved by inkjet printing a concentrated dye solution over the TiO_2 film, which produces solar cells with equal performance and stability as obtained with the popular dye drop casting method. In addition to allowing precise control of the dye loading required for dispensing just the right amount of dye to reach uniform, full coloration of the TiO_2 films without any need for washing off excess dye, the inkjet printing makes it also possible to freely adjust the amount and position of the dye to create DSSCs with tailored transparency, color density gradients, and patterns of one or more dyes on the same electrode. The method was confirmed applicable also for non-transparent, high-efficiency DSSC designs that employ a light scattering layer. The inkjet-dyed DSSCs exhibited high stability, retaining almost 100 % of their conversion efficiency (η = 6.4 ± 0.2 %) and short circuit current density (J_{SC} = 14.2 ± 0.6 mA/cm^2) when subjected to 1000 h accelerated aging test at 1 Sun illumination at 35 ºC, followed by additional 1154 hours at 0.5 Sun at 60 °C. These results overcome one of the main hurdles of realizing fully printed DSSCs and open opportunities for entirely new DSSC designs.

1. Introduction

Dye sensitized solar cells (DSSC) have been considered as a promising photovoltaic technology because they can be produced from abundantly available raw materials on various substrates using fast printing processes [1-3], and have intrinsic features, such as semi-transparency and color [4, 5], as well as good operation at low light intensity [6], which offer interesting product opportunities for building integrated photovoltaics and energy harvesting for low power wireless electronics [5, 7-9]. However, in order to manufacture them at high speed and with the roll-to-roll printing methods, some of their conventional fabrication steps have to be re-designed [1].

In the conventional fabrication method of dye-sensitized solar cell, a monolayer of dye molecules is attached to the nanocrystalline TiO_2 photoelectrode film by soaking it for 16 - 24 hours in a dye bath containing the sensitizer molecules, usually the ruthenium complex N719, which is followed by rinsing off the excess dye [10-11]. Although suitable for small scale experiments, and therefore popular in the research labs, this process is too slow for high through-put manufacturing, which should ideally consist of only fast, additive material printing and deposition steps, each completed in the timeframe from seconds to minutes, as already demonstrated for roll-to-roll fabrication of organic solar cells [12-17].

Studies show that the time required for saturating the surface of the TiO_2 with the N719 dye can be shortened down to three minutes [18] either by using a more concentrated dye solution [18-20], performing the sensitization at higher temperature [20,21], or by facilitating the supply of the dye molecules from the solution into the mesoporous film by circulating [20-22] or sonicating [23] the dye solution, by applying electrical field [26], or even by mixing the TiO_2 nanoparticles into the

concentrated dye solution followed by spraying [25]. The adsorption kinetics depend also on the chemical conditions of the TiO_2 surface, which can be altered more favorable for the dye adsorption by treating it with acidic solution [26]. For small area DSSCs, the fastest reported uptake of N719 through the soaking process was completed in 5 - 10 minutes using drop casting and pumping methods, which gave dyed TiO_2 photoelectrodes capable of producing 11 - 18 mA/cm^2 short circuit current density at the standard reporting conditions [18-20].

On the other hand, the sensitization studies of large surface area DSSC modules are few, and among them the popular scheme has been the dye circulation through a pump [21, 22, 27], however, the sensitization time through this circulation technique was long (more than two hours). In the case of the new concept of pre-sensitization of TiO_2 nanoparticles in the dye solution followed by spraying, reported recently for large area flexible DSSCs, material consumption may be an issue since a significant fraction of the sprayed material can be wasted over the non-active area, which can increase the overall production cost [24].

Since most of the active materials of DSSC can be deposited by printing and coating [1, 28], it would be advantageous from the point-of-view of manufacturing if also the dye could be simply printed on the TiO_2 films. The first steps to this direction were taken by Nazeeruddin et al. who introduced a rapid sensitization technique, in which a known volume of a highly concentrated N719 dye solution is pipetted onto the TiO_2 electrodes, or the electrode is immersed in it briefly [18]. This process, which took only three minutes at shortest [18], was thereafter followed by others who showed that the similar performance can be achieved with fast sensitization as with the traditional sensitization technique [19, 20, 29]. Nevertheless, in some of these studies, the excess, non-adsorbed dye was washed away afterwards [18, 29], which suggests that the control of the applied amount of dye was not sufficiently accurate to dispense just enough dye to saturate the film, but not more.

Clearly, the rapid sensitization could reach its full potential as a DSSC fabrication process only if it could be performed with a precise, automated and industrially scalable printing technique.

Here, we report a versatile dye sensitization process, achieved through the inkjet printing of concentrated dye solutions over the TiO_2 electrode films (Figure 1), which allows accurate control of the printed amount of dye, while producing solar cells with equal performance and stability as obtained with the known drop casting process. Based on a piezo-electric 'drop-on-demand' deposition of nominal 10 pico-liter sized droplets, the inkjet printing not only allows dispensing the right amount of dye needed for uniform, full coloration of the TiO_2 films without excess dye, but makes it also possible to freely adjust the dye loading to create solar cells with tailored transparency, color density gradients, and arbitrary patterns of one or multiple dyes on the same TiO_2 electrode (Figure 1).

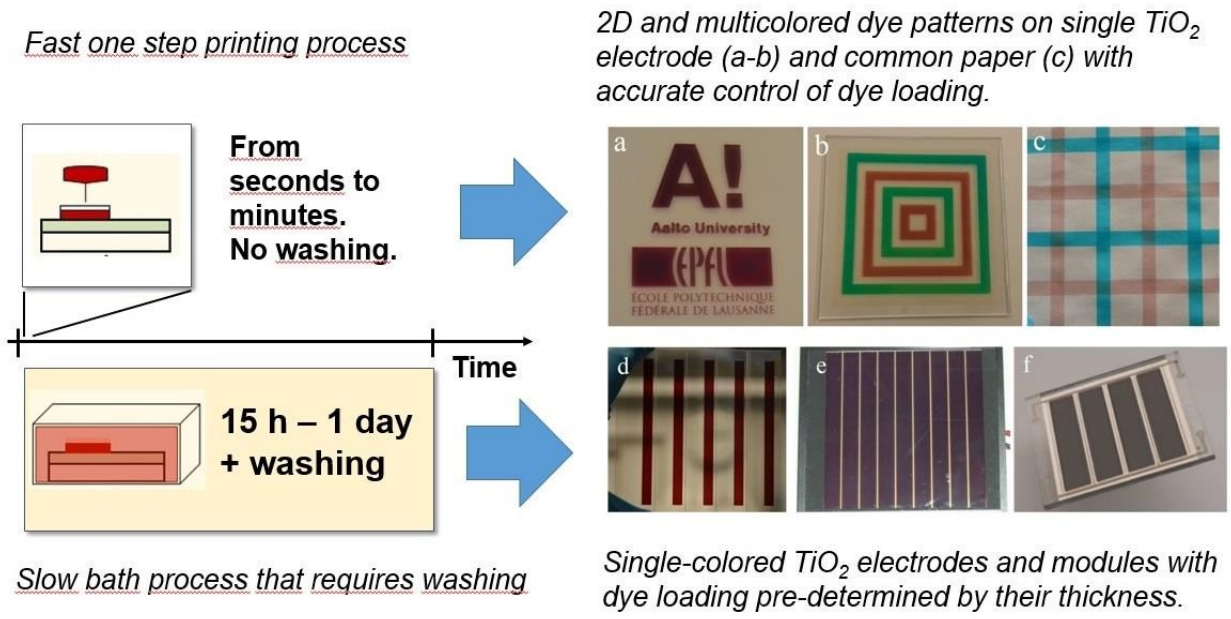

Figure 1. An Illustration of DSSC fabrication with old and new dye sensitization method a) 2D patterning demonstration of Aalto University and EPFL University logos with the inkjet printing technique used in this study from a concentrated dye solution of C101 dye over nanocrystalline TiO_2 layer b) colorful patterns (SQ2 dye in green and Z907 dye in red) can be obtained on single substrate which cannot be realized with old dye bath technique c) overlapping prints of SQ2 and Z907 dyes on regular office paper as a demonstration of co-sensitization and color tuning d-f) large area sensitized electrode with the traditional dye bath methods [30, 31].

The dye was printed with an automated inkjet printer (Fuji Film's Dimatix Material Printer, model DMP-2800 Series) by filling the concentrated dye solutions (10-16 mM in DMF or DMSO) into its polymer cartridge after passing them through a 0.2 μm filter (see the experimental section for further details). In the following, we discuss first the results from semi-transparent DSSCs, obtained by the inkjet printing of ruthenium sensitizer C101 [32]

2. Results and discussions

The following discussion has been divided into two parts (Section 2 and 3). In the first part, we demonstrated the potential capabilities of inkjet printing by using the semitransparent DSSCs produced through efficient control of dye loadings on nanocrystalline mesoporous TiO_2 layers (no scattering layers were employed) whereas in the second part, the stability of printed dye is investigated in the standard DSSCs employing the scattering TiO_2 layers.

2.1. Demonstration of the capabilities of inkjet printing of the dye

2.1.1 Variable transparency, color density gradients and multi-dye patterns in a single DSSC

One of the advantages of the inkjet printing is the controlled dispensing of fluid through which the dye loading of the photoelectrode can be accurately controlled. To demonstrate this capability, and to determine the printing parameters that yield full coloration, a 10 mM solution of C101 dye in DMF was inkjet-printed 1 - 5 times (1.1 μL/cm^2 per print) over a 7 μm thick TiO_2 electrode (0.4 cm^2, without a scattering layer) using 10 pL drop volume and 30 μm drop spacing, which corresponds to 11.3 nmol/cm^2 of dispensed dye per print. After a settling period of ca. 1 minute, during which the dye attached on the TiO_2 surface from the printed solution, the films were rinsed with DMF ("washed" samples) to remove possible non-adsorbed dye, or the rinsing step was omitted ("non-washed" samples). The photoelectrodes were then prepared to fully sealed solar cells (see the experimental section) and their optical transmittance and absorptance (Figure 2 a-d),

dye loading (Figure 3 a) and photovoltaic performance (Figure 4 a-f) was measured. Reference samples were prepared with the conventional 'rapid sensitization" by spreading 70 - 80 μL (175 - 200 μL/cm^2) of the same dye solution on an identical TiO_2 film with a pipette ("drop-cast" samples), followed by the same 15 minutes settling and final rinsing as done for the washed inkjet-printed samples.

According to the optical characterization, five printing cycles was enough to bring the coloration of the films close to that of the drop-cast samples, which we consider to be fully saturated with the dye. With 1 - 5 printing cycles, the device transmittance could be varied systematically from 38 % to 8% (at 550 nm), while the photoelectrode absorptance ranged correspondingly from 44% to 88% (Figure 2 a, d and Figure S3 in ESI). This immediately shows the unique feature of dye-sensitization with the inkjet-printing that could be interesting for many applications of the semi-transparent DSSCs: the transparency of the devices can be fine-tuned by the dispensed amount of dye without changing the thickness of the TiO_2 film. This is exactly opposite to the conventional dyeing processes that produce fully dye-saturated films with transmittance dictated by their thickness.

The other interesting feature of the inkjet printing already mentioned, is that it allows printing almost arbitrary dye patterns (Figure 1). Figure 2 g shows this capability in more detail by demonstrating the two most obvious opportunities it implies: the creation of dye patterns with varying color density ("gradient DSSC") and combinations of multiple dyes ("two-color DSSC") on the same photoelectrode. The optical characteristics of the five individual segments in the gradient DSSC, dyed with 1 - 5 prints of the C101 dye, are similar to those observed in the small individual DSSCs, but produced on the same long TiO_2 electrode stripe (Figure 2 b, e *vs.* a, d). In

the two-color DSSC, characteristic absorptance spectra of the printed red (C101) or black (N749) dyes can be distinguished from the adjacent segments without any signs of mixing between them (Figure 2 c, f). This shows that the inkjet printing accurately fixed the dyes in their own segments, allowing multicolored dye patterns to be produced on the same electrode. Note how uniform the coloration is in each segment of the two-color DSSC (Figure 2 g), and how repeatable the color density is between them, especially for the red dye (Figure 2 c and f). Although the coloration is less uniform in the gradient DSSC with 1 - 3 prints, it improves substantially with the successive 4^{th} and 5^{th} prints, and is remarkably good in the small DSSCs, even with a single print, so that practically no visual difference can be seen between the five times printed and drop-cast samples (Figure 2 g).

2.1.2 Precise control of the dye loading

Washing the TiO_2 films after printing the dye affected neither their optical absorptance nor visual appearance (Figure 2 d and g), and no traces of dye could be seen in the transmittance spectra recorded from the free electrolyte region of the cells (Figure 2 a, b and c). This indicate that all the printed dye had attached well to the TiO_2 film, leaving no excess or loosely bound dye that could be removed by washing or release into the electrolyte when built to a DSSC, even when the washing step had been omitted. The dye loading in the TiO_2 films, estimated from the photoelectrode absorptance spectra as detailed in the ESI, confirms this by showing excellent agreement between the washed and non-washed samples (Figure 3 a). Moreover, the dye loading increases linearly with the number of prints, demonstrating good control and repeatability of the printing process. The average dye loading per print determined from the slope of the linear fits is 11.2 nmol cm^{-2} in the washed and 11.7 nmol cm^{-2} in the non-washed samples, which matches almost perfectly with the dispensed amount (11.3 nmol cm^{-2}) determined by the printer settings (drop volume, spacing, and concentration). Note that the dye loading obtained with five prints (56

- 65 nmol cm^{-2}) is only slightly below the values reached with the drop-casting (68 - 81 nmol cm^{-2}), as one would expect if the loading does not exceed the saturation limit, but is close to it (Figure 3a). Similar results with excellent linearity are observed also in the gradient DSSC, although at somewhat higher 14.8 nmol cm^{-2} loading per print (Figure 3b). The relatively high values with five prints (74 - 79 nmol cm^{-2}), reached without signs of saturation in the linear trend, indicate somewhat higher film thickness in the gradient DSSC compared to the small DSSCs.

To confirm these results, some of the inkjet-dyed TiO_2 films from the same batch as those built to solar cells underwent a dye desorption experiment, where the printed dye was detached from the films to a desorption solution of known volume and then quantified with UV-VIS absorbance spectroscopy (see Experimental section and ESI). The results correspond well to those determined optically from the complete DSSCs: the dye loading increases linearly with the number of prints with slopes of 9.1 nmol cm^{-2} per print in the washed and 12.5 nmol cm^{-2} per print in the non-washed samples (Figure 3 c), and the values per film thickness obtained with five prints (respectively 6.5 and 8.9 nmol cm^{-2} μm^{-1}) are close to the values reported for the same dye by others (8.8 to 11.4 nmol cm^{-2} μm^{-1}) [33]. Note that, although the lower slope would suggest that the washing had removed significant amount of dye from the films in this case, only small amounts (< 6 nmol cm^{-2}) were detected in the five times printed samples with the UV-VIS spectroscopy, and none in the samples printed 1 - 4 times (data not shown). We therefore consider that these lower loadings, which deviate from the general trend more than the normal variation, resulted from occasionally failed printing cycles, which occurred in less than 4 % of all the 174 printing cycles constituting the results of Figures 3 a-c. Indeed, only four of the nine washed samples in the Figure 3 c show result below the linear trend of the non-washed ones, whereas the rest are matching well with it.

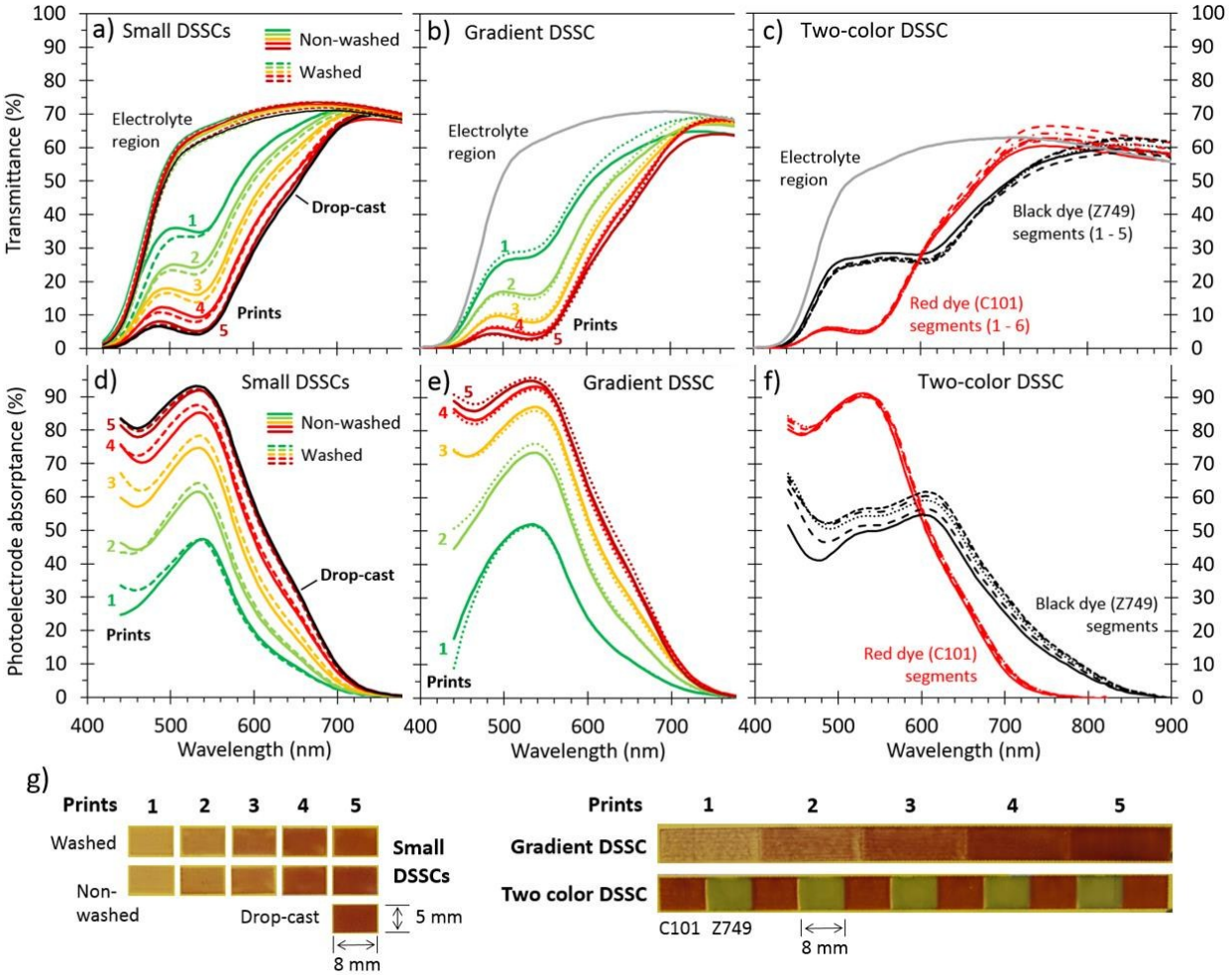

Figure 2. Optical characteristics of semi-transparent DSSCs with inkjet-printed dye: (a-c) transmittance, (d-f) photoelectrode absorptance, (g) photographs. (a, d) Small DSSCs dyed by inkjet-printing a dye solution (10 mM C101 in DMF) 1 - 5 times (1.1 μL/cm^2 per print) over a 7 μm thick TiO_2 electrode (0.4 cm^2, no scattering layer), followed by rising with DMF ("Washed") or omitting the rinsing ("Non-washed"), compared with a reference sample dyed by drop-casting 70 - 80 μL of the same dye solution on an identical TiO_2 film with a pipette, followed by the same washing treatment ("Drop-cast"). (b, e) A DSSC with color density gradient made by inkjet-printing the C101 dye solution 1 - 5 times over different parts of the same TiO_2 electrode. (c, f) A two-color DSSC with ink-jet printed red (C101) and black (N749) dye segments on the same TiO_2 electrode. Figures (d-f) show the internal absorptance spectra of the photoelectrode layer calculated as the ratio of the transmittances through the photoelectrode and electrolyte regions of the same cell (a-c), normalized to zero at long wavelengths (at 800 nm for C101 and 900 nm for N749); (g) photographs of the photoelectrode regions of the measured DSSCs taken with white backlight. The printing was done in all the cases with 10 pL drop volume and 30 μm drop spacing, using 10 mM C101 in DMF as the red dye ink and 10 mM N749 in DMF as the black dye ink (printed in 5 cycles). The small DSSCs spectra shown are examples from the complete data set consisting of three samples of each type. The complete data set and details on the calculation of figures (d-f) are available as ESI.

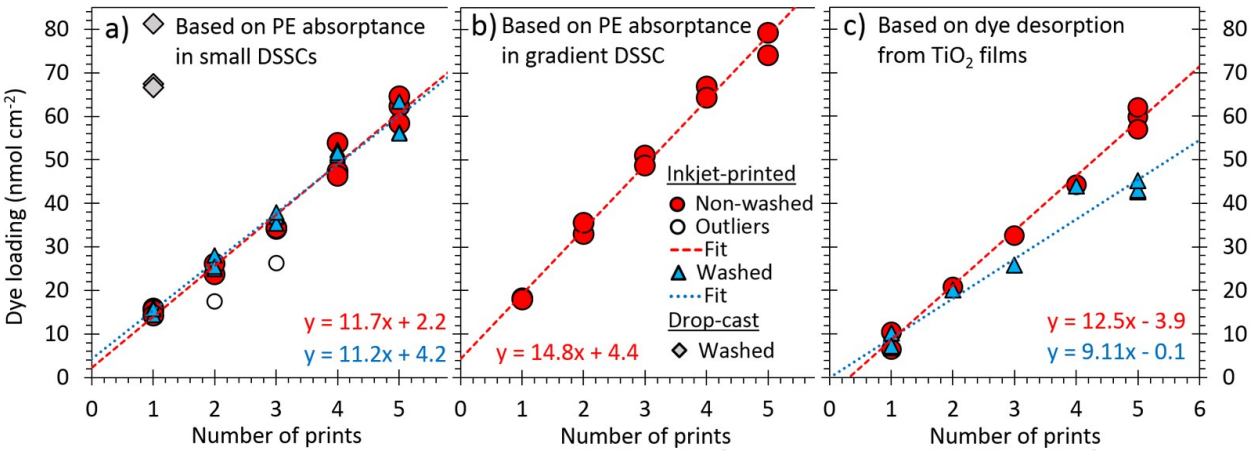

Figure 3. Dye loading in the small DSSCs (a) and the gradient DSSC (b) determined from their photoelectrode absoptance spectra shown in Figure 2, and confirmed by dye desorption from the TiO_2 films (c). The lines are linear fits to the data with equations shown. Note that many data points are overlapping. The number of data points are: (a) three for each 1 - 5 prints, (b) three for 1 and 3 prints and one for 2 to 4 prints, (c) two for each for each 1 - 5 prints. The data points marked as outliers in figure (a) correspond to samples with less uniform coloration and are excluded from the fit. Details on the dye loading calculations are given in the ESI.

2.1.3. Photovoltaic performance of the semi-transparent DSSCs

Also the results from the photovoltaic characterization show clear trends without any significant differences between washed and non-washed samples (Figure 4). The short circuit photocurrent density (J_{SC}) increases systematically with the number of prints, reaching ca. ~ 10.1 mA cm^{-2} with five prints (Figure 4 a), which is slightly lower than in the drop-cast samples (ca. ~ 11.4 mA cm^{-2}), as expected from their lower dye loading (Figure 3 a). The peak value of incident-photon-to-collected-electron efficiency (IPCE), and the energy conversion efficiency (η) similar trends as J_{SC}, reaching respectively 59 % and 5.1 % with the fifth print, compared to 65 % and 5.5 % with the drop-casting (Figures 4 b-c). This shows that the dye loading (light absorption) was the main performance determining factor of these cells, which is reflected also in the other JV characteristics: When more dye is printed in the TiO_2 film of fixed thickness, the open circuit voltage (V_{OC}) increases (Figure 4 d), because more photocurrent is generated per unit volume of the film while the recombination rate ('dark current') remains more or less constant. The same would happen if the light intensity was increased instead [34]. Finally, the fill factor (*FF*) and cell

resistance (R_{CELL}) follow qualitatively what is expected based on the evolution of J_{SC} and V_{OC} according to the electrochemical device model of DSSCs [34]: The decrease of *FF* (Figure 4e) follows the increase of J_{SC}, because the voltage losses caused by the internal cell resistances at the maximum power increase proportionally to the current density, whereas the dependence of V_{OC} on the photocurrent is weaker (logarithmic). On the other hand, the observed reduction of R_{CELL} (Figure 4f) with the increasing number of prints is expected based on the concomitant increase in V_{OC} (Figure 4d), because the recombination resistance of the photoelectrode, which is the main contributor to R_{CELL} at the open circuit, is a decreasing function of voltage [34].

Short circuit current densities measured from the individual segments of the gradient and two-color DSSC show the synergic operation that is expected from their electrical parallel connection in the cell: the lower J_{SC} of the more transparent segments are compensated by the higher J_{SC} from the darker segments, so that their average is close to the value measured for the solar cell as a whole (Figure 5). Note that the J_{SC} values of the five times printed red segments in both cells are lower than in the small DSSCs (Figure 4 a), although their optical absorption is similar (Figure 2 d-f). This is at least partly due to the difficulty of establishing comparable measurement conditions when most of the active area in the large cells has to be masked when the individual segments are measured. It also creates a situation where the results correspond to the parallel connection of illuminated and dark segments, making detailed JV analysis not feasible.

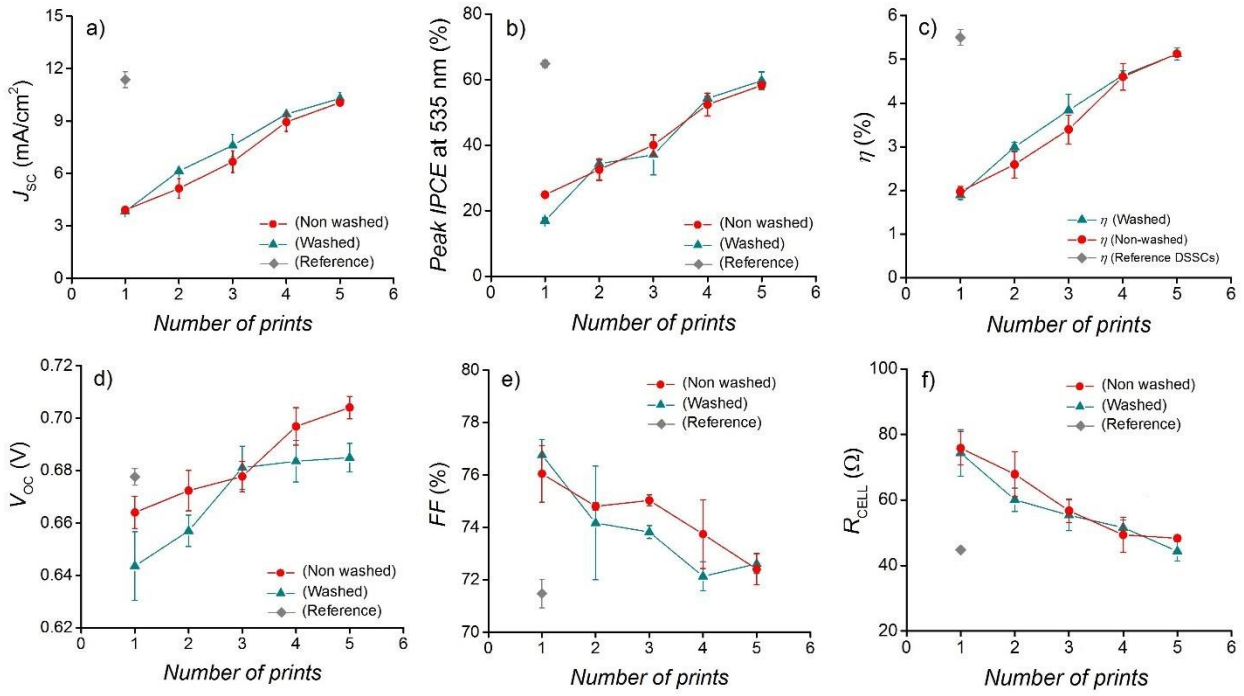

Figure 4. (a-f): Photovoltaic parameters of one batch of DSSC devices with 1 - 5 times printed PEs. The points are average values of three cells and the error bars represent their standard deviation.

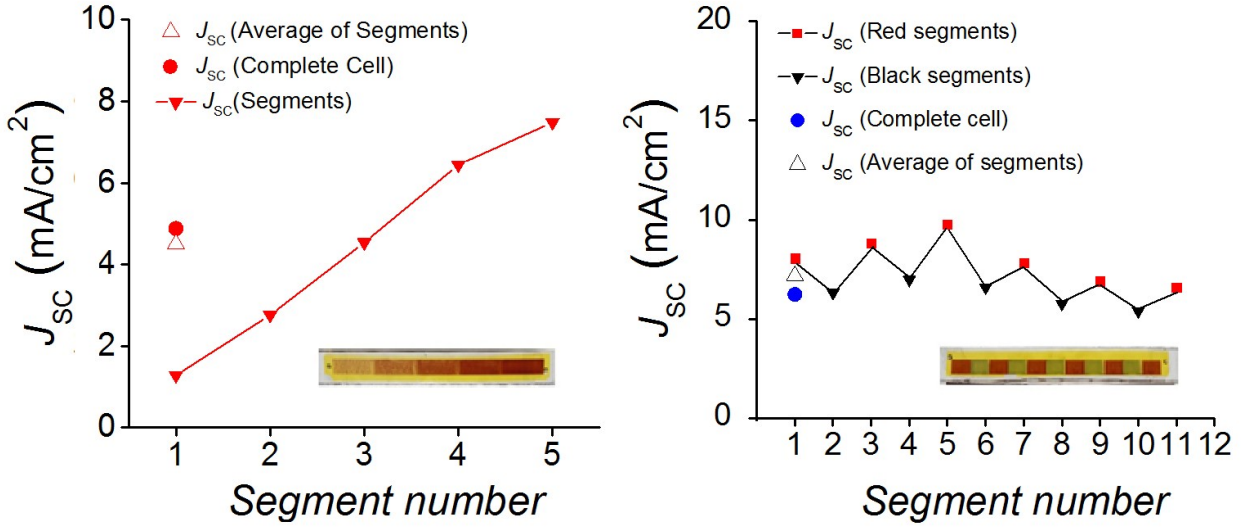

Figure 5. J_{SC} characteristics of the gradient and two-color DSSC.

2.2. Verification of high performance and stability of the inkjet-dyed DSSCs

Keeping all the above advantages and capabilities of the dye-sensitization by inkjet printing in mind, it was confirmed that it is entirely applicable also for the preparation of traditional, non-transparent, high-efficiency DSSC designs. For this purpose, photoelectrodes consisting of ~ 12 µm thick mesoporous TiO_2 layer and a 4 - 6 µm thick light scattering TiO_2 layer (0.8 x 0.5 cm^2 PE area) were sensitized by dispensing 5 ± 1 µl volume through 5 prints, which exhibited very minor impressions of excess dye over the TiO_2 scattering layer, and were not rinsed further with the solvent.

The complete DSSCs were fabricated with these dye-printed photoelectrode by employing a sulfolane - ionic liquid electrolyte (coded as Z988) [6] as the redox mediator along with platinum (Pt) counter electrodes, and their initial and long term stability performance was compared with the reference DSSCs, which were fabricated by drop casting the known volumes (70-80 µl with 20-25 minute settling) of concentrated (10 mM in DMF) solution of the C101 dye over the similar PEs, followed by washing with DMF, using current-voltage (JV) analysis, electrochemical impedance spectroscopy (EIS) and incident photon to collected electron (IPCE) measurements.

Statistical analysis of the average initial performance of seven dye-printed DSSCs (efficiency 6.4 ± 0.3 %) and five reference DSSCs (6.2 ± 0.4 %) showed no statistically significant difference between the two groups for any of the JV or EIS parameters (Table 1 and 4 in the ESI, respectively). Most importantly, the two types of DSSCs showed almost equal short circuit current densities (14.0 ± 0.2 mA/cm^2 for printed dye and 13.8 ± 0.3 mA/cm^2 for reference DSSCs), which confirms the successful sensitization process through inkjet printing.

The best performing devices from printed dye based DSSC (five cells) and reference DSSCs (three cells) were then monitored through an accelerated ageing test under 35 ºC along with 1 Sun

illumination over a period of 1000 hours (see the experimental section and ESI for further details). Figure 6 a-e represents the ageing trends of the photovoltaic parameters that were collected from periodic measurements during the 1000 h test, and the initial and aged JV and IPCE curves of the best DSSCs of each type are shown in Figures 7 and 8 respectively. The results reveal highly stable performance retained at almost 100 % of the initial conversion efficiency (η = 6.4 ± 0.2 %) and short circuit current density (J_{SC} = 14.2 ± 0.6 mA/cm^2) values, with no statistically significant ageing of any of the JV parameters of each cell type, according to a paired Student's t-test at 95 % confidence (see ESI). This was also confirmed with periodic electrochemical impedance spectroscopy measurements performed throughout the ageing test, which revealed high stability with no statistically significant changes in any of the internal resistance components of the DSSC (Figure 9 a and b, see ESI for detailed results). The only statistically significant difference observed was a 5 % lower V_{OC} in the printed cells compared to the reference cells at the end of the aging period (1000 h, ESI Table 2), and correspondingly 14 % lower recombination resistance in the printed cells, as measured by EIS at V_{OC} (ESI Table 5). This points to a small difference in the aging behavior of the TiO_2/dye/electrolyte interface, which however, due to a compensating evolution of J_{SC} (Figure 6 d), resulted to no difference in the overall efficiency (Figure 6 d). Very small impressions of excess dye that had remained over the scattering TiO_2 layer after the dye printing step, slowly dissolved into the electrolyte during the accelerated ageing test, which however caused no effects on overall cell performance.

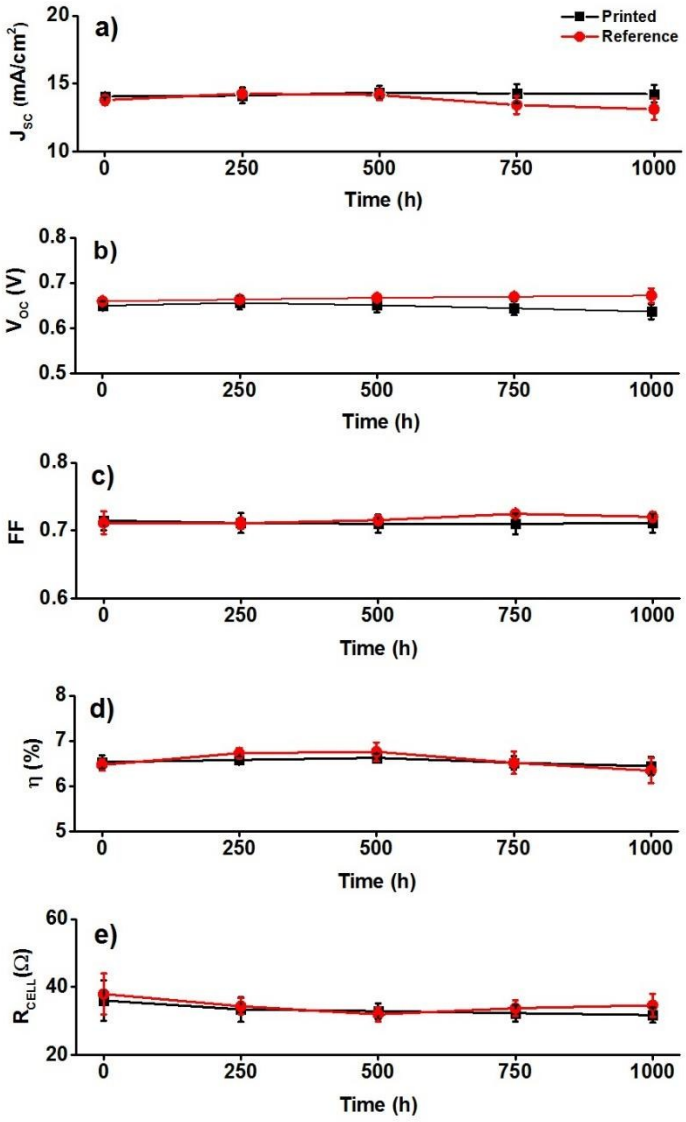

Figure 6 (a-e): Photovoltaic parameters of fabricated devices of each type of DSSC obtained with periodical measurements during an accelerated ageing test (at 35 ºC and 1 Sun illumination) for a period of 1000 hours. The points are average values of five printed and three reference (drop-casted) cells, and the error bars represent standard deviation.

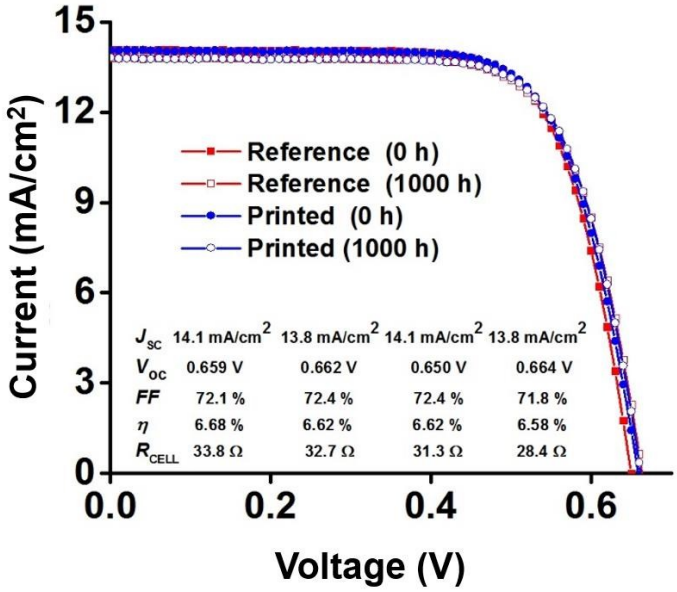

Figure 7. Initial and aged (at 35 °C and 1 Sun illumination) JV curves of the best DSSCs of each type used in this study.

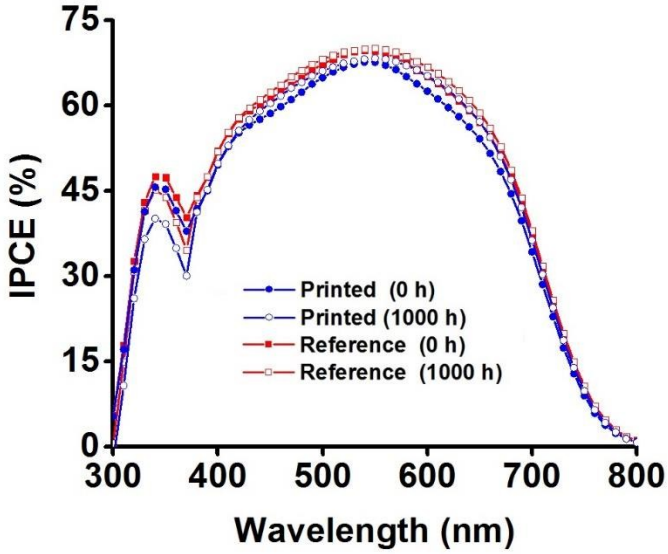

Figure 8. Initial and aged (at 35 °C and 1 Sun illumination) IPCE spectra of the best DSSCs of each type used in this study.

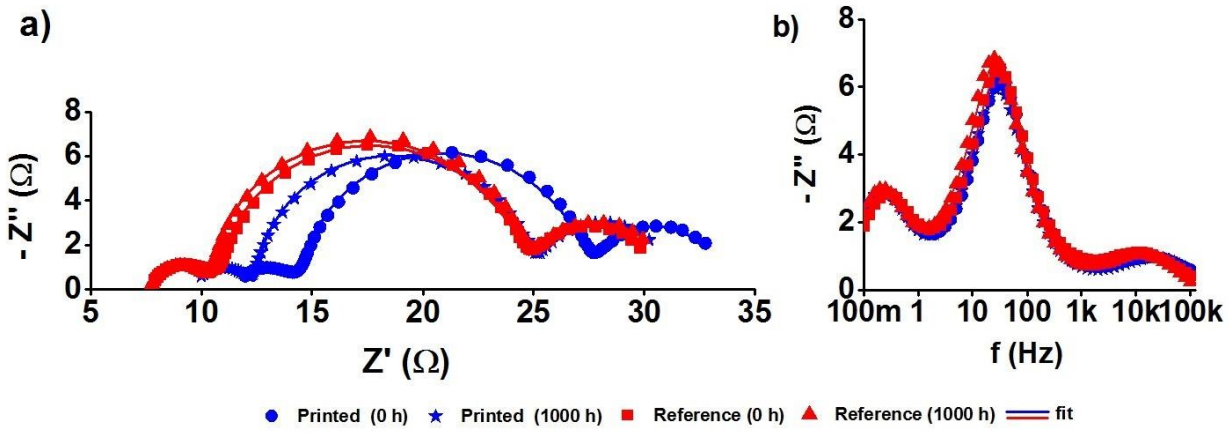

Figure 9. Typical fresh and aged EIS spectra of complete DSSCs of the best devices of each type used in this study with Pt counter electrode (a) Nyquist plots, (b) imaginary impedance (Z") vs frequency. The solid lines represents the fitted data whereas the points represents the measured data. The shift of the Nyquist plot along the real axis in case of printed dye DSSC was due to gradual decrease in the contact (series) resistance of the silver paint during the aging test.

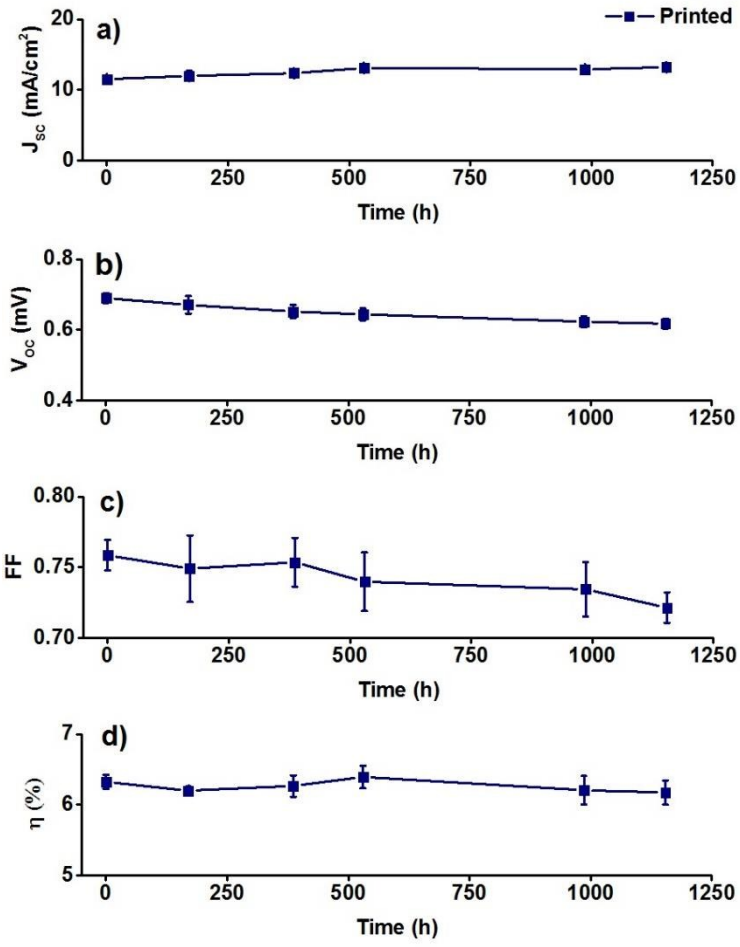

Figure 10 (a-d): Photovoltaic parameters of fabricated devices of each type of DSSC obtained during the periodical measurements during an accelerated ageing test (at 60 ºC and half Sun illumination) for a period of 1184 hours.

Encouraged by the first promising long term stability test, the same dye printed DSSCs (five cells) were further subjected to an additional accelerated test that was conducted at half Sun illumination at higher temperature (60 °C) for 1154 more hours (to test if a higher temperature could affect the performance). Again the solar cells exhibited stable performance retaining almost 100 % of the initial conversion efficiency (Figure 10 a-d). Hence these two ageing tests certifies the potential of inkjet printing as a new sensitization process for DSSCs which is expected to be developed further after these results.

In addition to the main capabilities of inkjet printing the dye discussed earlier, namely the controlled dispensing and patterning of the dye, several other possible advantages can be mentioned. For instance, the highly pure dye solution can be contained in the printer cartridge until dispensed on the active layer, which protects it from contamination or degradation. Since the dye is printed only on the active layer, additional cleaning steps to remove the dye from the non-active area around it, before the application of the thermoplastic sealants, are not necessary. For the same reason, the inkjet printing may also be potentially beneficial for plastic photoelectrodes, because it provides an opportunity to minimize the contact and interaction of possibly harsh solvents with the plastic substrates, such as the commonly used indium doped tin oxide coated polyethyleneterephtalate (ITO-PET) and polyethylenenaphtalate (ITO-PEN) sheets. For example, ITO-PET might swell when exposed to certain solvents such as acetonitrile for the long time periods required in the traditional dye bath soaking process. Hence we also aim to apply and investigate this technique on flexible PEs in future. Again, unlike in the dye circulation process used for sensitizing the hermetically pre-sealed modules, in the inkjet printing the dye solution never comes in contact with the Pt catalyst, which may help keep it clean of adsorbed dye molecules that could lower its catalytically active surface area. Moreover, the inkjet printing of dyes can also be potentially utilized for more accurate and controlled co-sensitization of TiO_2

layers by multiple dyes, by printing them at optimized amounts over the same electrode area, instead controlling only the soaking time, which is the traditional approach.

4. Conclusion

In conclusion, the TiO_2 photoelectrodes of the dye-sensitized solar cell (DSSC) can be effectively stained by inkjet printing concentrated dye solutions on them. The unique feature of the inkjet printing is that it allows accurate control of the dye loading with respect to both the amount and position on the TiO_2 film. This offers several advantages over the conventional dye application methods. First, close to full coloration can be reached without rinsing off any excess dye, which simplifies the DSSC fabrication process and reduces material consumption. Second, the color density of the films can be tuned without changing their thickness, which offers a new degree of freedom in the design of semi-transparent DSSCs for example for building integrated photovoltaics. Third, the high spatial resolution of inkjet printing makes it possible to create color density gradients and patterns of multiple dyes on the same photoelectrode, which suggests a new avenue for creating multi-colored DSSC designs attractive for example for stylish product integration of DSSCs. The inkjet printing of the dye is applicable with or without a light scattering TiO_2 layer, and yields stable devices with performance equal to those prepared with the manual drop casting sensitization process. Since the inkjet printing is one of the most well-known, established and scalable printed electronics manufacturing technique, this new dye-sensitization process could be readily adopted in the industrial settings, possibly even in high throughput roll-to-roll production of flexible DSSC devices. Combined with our previously reported inkjet printing of the electrolyte [36], the results presented here show a path towards fully inkjet-printed DSSCs.

5. Experimental

Materials

Chloroplatinic acid hydrate ($H_2PtCl_4 \cdot 6H_2O$, purity 99.9 %), Guanidine Thiocyanate (GuSCN, purity > 99 %), 1-Methylbenzimidazole (NMBI, purity 99 %) and all the solvents (Sulfolane 99 % purity, 2-Propanol 99.5 % anhydrous, Acetonitrile 99.8 % anhydrous, N, N Dimethylformamide (DMF) 99.8 % purity) and Titanium(IV) chloride tetrahydrofuran complex were obtained from Sigma Aldrich. 1, 3-dimethylimidazolium iodide (DMII), 1-Methyl-3-Propylimidazolium (PMII > 98 % purity), 1-ethyl-3-methylimidazolium iodide (EMII > 98 % purity) and 1-ethyl l-3-methylimidazolium tetracyanoborate (EMITCB) were purchased from Merck. TiO_2 nanocrystalline paste (18-NRT, 20 nm) and TiO_2 scattering paste (WER 2-0, 400 nm) were purchased from Dyesol. Dye C101 and Electrolyte 'Z988' were produced as reported earlier [6, 32, 35]. Dyes N749 and SQ2 were obtained from Solaronix whereas dye Z907 was purchased from Dyesol. Solvent Dimethyl Sulfoxide (DMSO, Ultra-pure grade) was purchased from Amresco.

TiO_2 photoelectrodes (PE)

The photo electrodes for this experiment were prepared as follows. Fluorine doped tin oxide (FTO) coated NSG-Glass substrates (area = 1.6 cm x 2.0 cm and sheet resistance 10 Ω/Sq) were first washed and sonicated with detergent (10 minutes). The substrates were further washed and sonicated with acetone and ethanol solvents (5 minutes each) and were dried with compressed air. These substrates were then placed and cleaned (15 minutes) in a UV-O_3 cleaner (Bioforce Nanosciences USA). After cleaning in UV-O_3 chamber, the substrates were immersed in 40 mM $TiCl_4$ solution and heated (30 minutes) in a preheated programmable oven and were sequentially rinsed with deionized water (DIW) and ethanol and were again dried with compressed air. The TiO_2 layers (12 µm of nanocrystalline TiO_2 particles, 20 nm and 4 µm thick layer of scattering particles, 400 nm) were sequentially screen printed and sintered at 450 ºC for 30 minutes in programmable oven and were cooled down to room temperature. Then the photoelectrodes were re-heated in the 40 mM $TiCl_4$ aqueous solution and were washed again with DIW and ethanol and

were dried with compressed air. Then the photoelectrodes were again sintered at 450 ºC in the programmable oven and were cooled down before the dye sensitization step. **Note:** The photoelectrodes for dye desorption test (Figure 3 a-b) and for the dataset of DSSCs presented in Figure 4 (a-f) were not subjected to any $TiCl_4$ treatment and were not having any scattering layers, but only the semi-transparent TiO_2 layer (thickness 7 µm).

Dye solution formulations for inkjet printing

In the case of red C101 and black N749 (Figures 1a, and 2 - 10) the dye solution were 10 mM in DMF. In the case of blue SQ2 and red Z907 dyes (Figures 1 b, c), stock solutions were prepared (for individual dye) by dissolving 45 mg of dyes (SQ2 or Z907) in 3 ml of solvent dimethyl sulfoxide (DMSO). Both DMF and DMSO were found suitable solvents for inkjet printing these dyes.

Details of inkjet printing of dyes

The dye printing was achieved with an automated inkjet printer (Fuji Film's Dimatix Material Printer, Model DMP-2800 Series, see Figure S4 in the Supporting Information) by filling the concentrated dye solutions (dye C101 and N749) into its polymer cartridge. Additionally, the cartridge is equipped with a so called 'print head' which consists of 16 micro-channels (orifices) through which the solution was dispensed. In order to get the good printing results, the dye solution was passed through a 0.2 µm filter as recommended in the operating instructions of the printer. The TiO_2 layers (actual area = 0.8 x 0.5 cm^2) without scattering layer were sensitized with both dye solutions at 10 mM concentration using 30 µm drop spacing leading 0.45 µL solution and 4.5 nmol of dye deposition per cycle. See Figure 2 caption for more details. The cells, which underwent the ageing study, were assembled employing a scattering layer on nanocrystalline TiO_2 and they were processed with 20 µm drop spacing corresponding to 1 µL solution and 16 nmol of dye per print from 16 mM solution. The printing process took around 3 min and 2 minutes for 20 µm and 30 µm drop spacing respectively.

Photoelectrode sensitization for reference DSSCs

The TiO_2 layers of the photoelectrodes for the reference DSSC were sensitized with similar procedure as reported earlier for quick sensitization of dye C101 [33]. In brief, the TiO_2 layers were completely covered by spreading dye solution of known volumes (70 µl) with similar concentration (10-16 mM of dye C101 dye in DMF) as used in inkjet printing of dye and were left for 20 minutes in a sealed plastic box. After that each photoelectrode was washed with DMF to remove excess dye and was dried with compressed air before the cell assembly.

Counter electrodes (CE)

A drop (4 µl) of 10 mM Chloroplatinic acid hydrate (H_2PtCl_4. $6H_2O$) solution (in 2 Propanol) was casted over pre-cleaned FTO coated glass substrates (TEC 7) and was fired at 410 ºC for 20 minutes. After that all the electrodes were cooled down to room temperature and were placed in a tightly sealed plastic box prior the final cell assembly.

Electrolyte composition

The ionic liquid electrolyte coded as Z988 with following composition was used for this study: DMII/EMII/EMITCB/I_2/ NMBI / GuSCN (molar ratio 12:12:16:1.67:3.33:0.67) mixed and diluted with 50 % of sulfolane (v/v).

Cell assembly

The cell channel was defined by separating PE and CE through a thick (25 µm) Surlyn frame foil. The ionic liquid electrolyte was introduced into the cell channel through the drilled holes at CE side. The cells were then sealed with 25 µm thick Surlyn foil and a thin glass cover. In last, the contacts were fabricated by applying the copper tape and quick drying silver paste at the non-active area of the electrodes.

Measurements

The JV curves of the DSSCs were recorded in a Xenon lamp based solar simulator (Peccell Technologies, Japan, Model PEC-L01) under 1000 W/m^2 light intensity calibrated to equivalent 1 Sun conditions with a reference solar cell (PV Measurements Inc.), by using a black tape mask (aperture area 0.17 cm^2). The electrochemical impedance spectra were recorded from 100 mHz to 100 kHz at the open circuit conditions under 1000 W/m^2 light intensity with Zahner-Elektrik IM6 electrochemical workstation, and analyzed with Zview2 software (Scribner Associates Inc.) using the well-known equivalent circuit model of DSSCs [34]. The incident photon to collected electron efficiency (IPCE) and transmittance spectra were measured with QEX7 Spectral response measurement unit (PV Measurements Inc.) at near normal incidence without bias light. The first stability test of the solar cells test was performed by keeping them for 1000 hours at open circuit conditions at 35 ºC in a self-made solar simulator under 1 Sun light intensity provided through halogen lamps (Philips 13117) and a UV filter (Asmetec GmbH, 400 nm cut-off), while recording their JV curves periodically in the abovementioned separate solar simulator (Peccell Technologies, Japan). The second stability test was executed in the Suntest CPS Plus system at 60 °C under half Sun light illumination and similar periodic measurements as mentioned above were performed to record the JV curves in the solar simulator. The dye loading (mol cm^{-2}) in complete solar cells was determined based on two transmittance measurements from each cell: one taken through the photoelectrode and one through the electrolyte filled edge region next to it. The dye loading in freshly sensitized TiO_2 films was determined by desorbing the dye in the mixed solution of TMAOH and DMF (50/50 by volume). The decadic molar attenuation coefficient of C101 dye (17.5×10^3 M^{-1} cm^{-1}) used in the calculations was taken from ref. (33). The details of both methods are given as ESI.

6. Acknowledgements

G. H. gratefully acknowledges Academy of Finland for the post-doctoral research fellowship. J. H. acknowledges the financial support from the Technology Industries of Finland Centennial Foundation (NIR-DSC project). M. G. acknowledges financial support from Swiss National Science Foundation and CTI 17622.1 PFNM-NM, glass2energy SA (g2e), Villaz-St-Pierre, Switzerland. This work was also supported by the SELECT+ (Environomical pathways for sustainable energy services). Bioeconomy infrastructure is also acknowledged for the use of the equipment.

7. References

[1] G. Hashmi, K. Miettunen, T. Peltola, J. Halme, I. Asghar, K. Aitola, M. Toivola, P. Lund, *Ren. Sust. Energy Rev.*, 2011, **15**, 3717-3732.

[2] A. Feltrin, A. Freundlich, *Ren. Energy*, 2006, **33**, 180-185.

[3] C. S. Tao, J. Jiang, M. Tao, *Sol. Energy Mater. Sol. Cells*, 2011, **95**, 3176-3180.

[4] A. Hinsch, W. Veurman, H. Brandt, K. Flarup Jensen, S. Mastroianni, *ChemPhysChem*, 2014, ***15***, 1076-1087.

[5] K. Zhang, C. Qin, X. Yang, A. Islam, S. Zhang, H. Chen, L. Han, *Adv. Energy Mater.*, 2014, **4**, 1301966.

[6] M. Marszalek , F. D. Arendse, J. D. Decoppet, S. S. Babkair, A. A. Ansari , S. S. Habib, M. Wang, S. M. Zakeeruddin, M. Grätzel, *Adv. Energy Mater.*, 2014, **4**, 1301235.

[7] Z. L. Wang, W. Wu, *Angew. Chem.*, 2012, **51**, 2 - 24.

[8] F. De Rossi, T. Pontecorvo, T.M. Brown, *Applied Energy*, 2015, **156**, 413-422.

[9] S. Vignati, *Comm. Syst. Dept., KTH, Master of Science Thesis*, 2012.

[10] S. Ito, T. N. Murakami, N. Takurou, P. Comte, P. Liska, C. Graetzel, M. K. Nazeeruddin, M. Graetzel, *Thin Solid Films.*, 2008, **516**, 4613-4619.

[11] M. K. Nazeeruddin, A. Kay, I. Rodicio, R. Humphry-Baker, E. Mueller, P. Liska, N. Vlachopoulos, and M. Graetzel, *J. Am. Chem. Soc.*, 1993 **115**, 6382-6390.

[12] M. Hösel, H. F. Dam, F. C. Krebs, *Energy Tech.*, 2015, **3**, 293-304.

[13] J. E. Carle, M. Helgesen, M. V. Madsen, E. Bundgaard, F. C. Krebs, *J. Mater. Chem. C.*, 2014, **2**, 1290-1297.

[14] D. Angmo, S. A. Gevorgyan, T. T. L. Olsen, R. R. Søndergaard, M. Hösel, M. Jørgensen, R. Gupta, G. U. Kulkarni, F. C. Krebs, *Org. Electr.*, 2013, **14,** 984-994.

[15] J. S. Yu, I. Kim, J. S. Kim, J. Jo, T. T. L. Olsen, R. R. Søndergaard, M. Hosel, D. Angmo, M. Jørgensen, F. C. Krebs, *Nanoscale.*, 2012, **4**, 6032-6040.

[16] J. Adams, G. D. Spyropoulos, M. Salvador, N. Li, S. Strohm, L. Lucera, S. Langner, F. Machui, H. Zhang, T. Ameri, M. M. Voigt, F. C. Krebs, C. J. Brabec, *Energy Environ. Sci.*, 2015, **8**, 169-176.

[17] K. Liu, T. T. Larsen-Olsen, Y. Lin, M. Beliatis, E. Bundgaard, M. Jørgensen, F. C. Krebs, X. Zhan, *J. Mater. Chem. A.*, 2016, **4**, 1044-1051.

[18] M. K. Nazeeruddin, R. Splivallo, P. Liska, P. Comte, M. Grätzel, *Chem. Commun.*, 2003, **12**, 1456-1457.

[19] I. Concina, E. Frison, A. Braga, S. Silvestrini, M. Maggini, G. Sberveglieri, A. Vomieroa, T. Carofiglio, *Chem. Commun.*, 2011, **47**, 11656-11658.

[20] P. J. Holliman, M. L. Davies, A. Connell, B. V. Velasco, T. M. Watson, *Chem. Comm.*, 2010, **46**, 7256-7258.

[21] M. Späth, P. M. Sommeling, J. A. M. van Roosmalen, H. J. P. Smit, N. P. G. van der Burg, D. R. Mahieu, N. J. Bakker, J. M. Kroon, *Prog. Photovolt: Res. Appl.*, 2003, **11**, 207-220.

[22] R. Sastrawan, J. Beier, U. Belledin, S. Hemming, A. Hinsch, R. Kern, C. Vetter, F. M. Petrat, A. P. Schwab, P. Lechner, W. Hoffmann, *Sol. Energy Mater. Sol. Cells.*, 2006, **90**, 1680-1691.

[23] Y. Seo, J. H. Kim, *J. Indust. Eng. Chem.*, 2013, **19**, 488-492.

[24] H. G. Han, H. C. Weerasinghe, K. M. Kim, J. S. Kim, Yi. B. Cheng, D. J. Jones, A. B. Holmes & T. H. Kwon, *Scientific Reports.*, 2015, **5**, 14645.

[25] B. Kim, Se W. Park, J. Y. Kim, K. Yoo, J. Ah Lee, M. W. Lee, D. K. Lee, J. Y. Kim, B. S. Kim, H. Kim, S. Han, H. J. Son, M. J. Ko, *Appl. Mater. Interfaces.*, 2013, **5**, 5201−5207.

[26] H. Seo, M. K. Son, I. Shin, J. K. Kim, K. J. Lee, K. Prabakar, H. J. Kim, *Electrochimica Acta.*, 2010, **55**, 4120 -4123.

[27] R. Sastrawan, J. Beier, U. Belledin, S. Hemming, A. Hinsch, R. Kern, C. Vetter, F. M. Petrat, A. P. Schwab, P. Lechner, W. Hoffmann, *Prog. Photovolt: Res. Appl.*, 2006, **14**, 697-709.

[28] S. G. Hashmi, T. Moehl, J. Halme, Y. Ma, T. Saukkonen, A. Yella, F. Giordano, J. D. Decoppet, S. M. Zakeeruddin, P. Lund, Michael Gratzel, *J. Mater. Chem. A.*, 2014, **2**, 19609-19615.

[29] S. C. Yeh, P. H. Lee, H. Y. Liao, Y. Y. Chen, C. T. Chen, R. J. Jeng, J. J. Shuye, *Sust. Chem. and Eng.*, 2015, **3**, 71−81.

[30] Figure 1e is reprinted from Current Applied Physics, vol 10, issue 2, H. Arakawa, T. Yamaguchi, T. Sutou, Y. Koishi, N. Tobe, D. Matsumoto, T. Nagai, Efficient dye-sensitized solar cell sub-modules, S157–S160, (2010), with permission from Elsevier.

[31] Figure 1f is reprinted from Progress in Photovoltaic Research and Applications, vol 18, H. Pettersson, T. Gruszecki, C. Schnetz, M. Streit, Y. Xu, L. Sun, M. Gorlov, L. Kloo, G. Boschloo, L. Haggman, A. Hagfeldt, Parallel-connected monolithic dye-sensitised solar modules¸ 340-345, (2010), with permission from John Wiley and Sons.

H. Pettersson, T. Gruszecki, C. Schnetz, M. Streit, Y. Xu, L. Sun, M. Gorlov, L. Kloo, G. Boschloo, L. Haggman, A. Hagfeldt, *Prog. Photovolt: Res. Appl.*, 2010, **18**, 340-345.

[32] F. Gao, Y. Wang, D. Shi, J. Zhang, M. Wang, X. Jing, R. H. Baker, P. Wang, S. M. Zakeeruddin and M. Gratzel, 2008, *J. Am. Chem. Soc.*, **130**, 10720-10728.

[33] M. Wang, S. Plogmaker, R. H. Baker, P. Pechy, H. Rensmo, S. M. Zakeeruddin, M. Gratzel, *Chem Sus Chem.*, 2012, **5**, 181 - 187.

[34] J. Halme, P. Vahermaa, K. Miettunen, P. Lund, *Adv. Mater.*, 2010, **22**, E210-E234.

[35] J. D. Decoppet, T. Moehl, S. S. Babkair, R. A. Alzubaydi, A. A. Ansari, S. S. Habib, S. M. Zakeeruddin, H. W. Schmidt, M. Gratzel, *J. Mater. Chem. A.*, 2014, **2**, 15972 - 15977.

[36] S. G. Hashmi, M. Ozkan, J. Halme, K. Dimic-Misic, S. M. Zakeeruddin, J. Paltakari, M. Grätzel, P. D. Lund, *Nano Energy.*, 2015, **17**, 206–215.

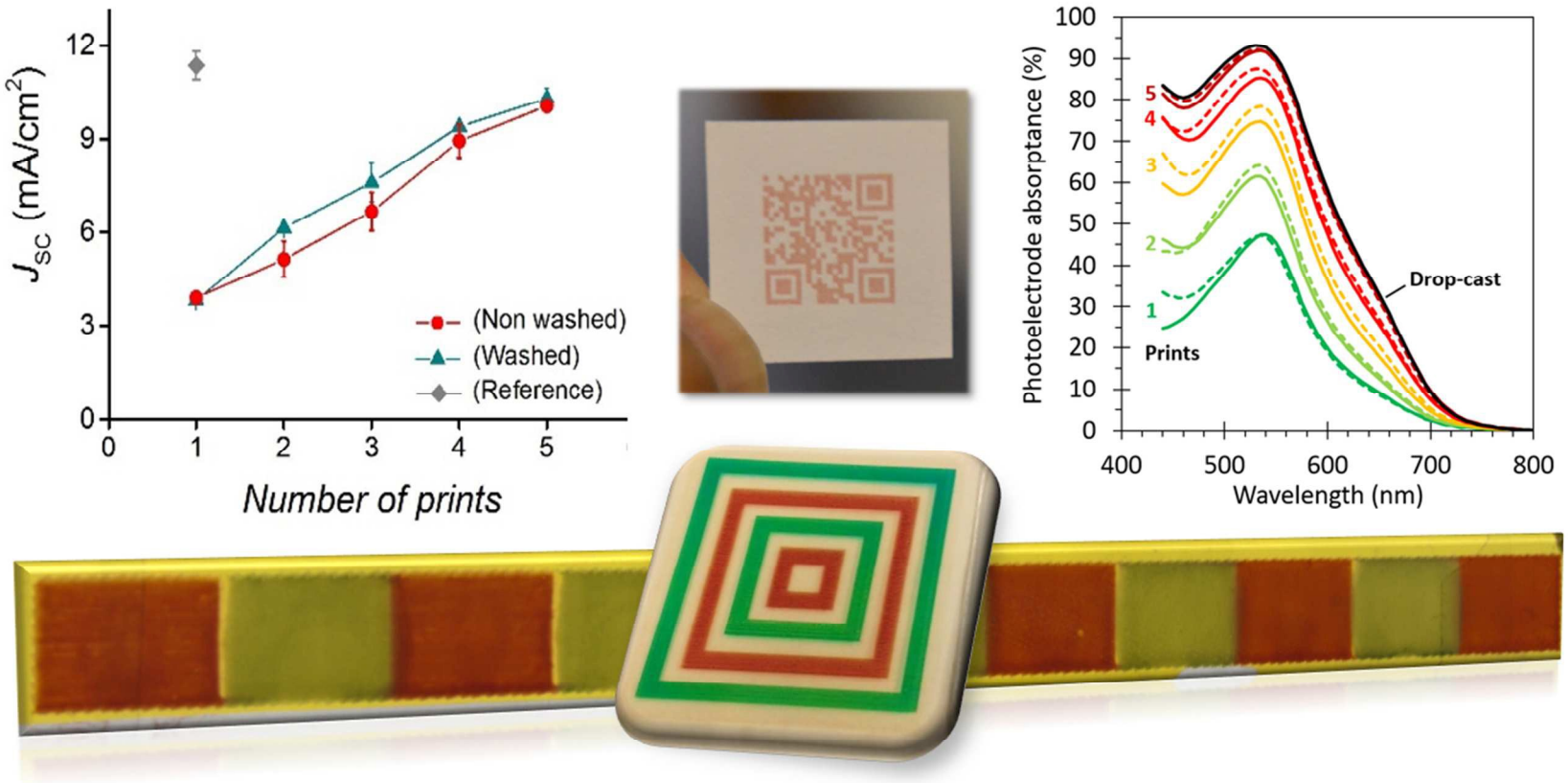

Inkjet printing dyes on TiO_2 films enables DSSCs with tailored transparency, color density gradients, and patterns of multiple dyes on the same photoelectrode.

Broader context

Dye-sensitized solar cells (DSSC) can be possibly produced at low cost with high throughput methods such as screen or inkjet printing, but to do so requires re-designing some of their conventional fabrication steps. One of them is the step where the light absorbing dyes are attached to the nanocrystalline TiO2 photoelectrode. This is normally done in the laboratory scale by slowly soaking the TiO2 film in a dye solution. Although methods exist to speed up the process from hours to minutes, it could be even quicker and consume less materials, if the dye could be simply printed on the TiO2 film. We report here for the first time, that this can in fact be done with inkjet printing, which at the same time bring about additional benefits. The inkjet dyeing not only simplifies the overall fabrication and consumes less solvents, but also opens new opportunities for creating multi-coloured solar cells with tailored transparency and decorative designs, which can be important attributes for the commercialization of DSSCs.